Available online at www.sciencedirect.com
SCIENCE DIRECT®
International Journal of Thermal Sciences 43 (2004) 901–914
International Journal of Thermal Sciences
www.elsevier.com/locate/ijts

Influence of side wall expansion angle and swirl generator on flow pattern in a model combustor calculated with k–ε model

S. Mondal [a], A. Datta [b], A. Sarkar [a,*]

[a] *Department of Mechanical Engineering, Jadavpur University Kolkata 700032, India*
[b] *Department of Power Engineering, Jadavpur University Salt Lake Campus, Kolkata 700098, India*

Received 3 June 2003; received in revised form 25 November 2003; accepted 6 January 2004

Available online 27 March 2004

Abstract

A numerical study based on finite difference solution technique is made to characterize turbulent isothermal (non-reacting) swirl flow in a combustor for varying side wall expansion angle and different types of swirl generators. A standard k–ε turbulence model with logarithmic wall function has been adopted for the closure. The differences in the flow patterns under various conditions are described through the overall streamline plots as well as by using the local variations of the mean and turbulent flow quantities. The central re-circulation zone has been identified as a critically important one in the combustors, and its detailed characterization, in terms of size, location and strength, has been made for the different parameters under study.

Keywords: Swirl combustor; Turbulent isothermal swirling flow; Swirl generator; Side wall expansion angle; Characteristics of recirculation zone

1. Introduction

Turbulent swirling flows in confined geometry is important because of their wide spread use in combustors, particularly in gas turbines, ramjet engines and industrial furnaces. It is established that the flow pattern plays an important role in controlling the combustion process by influencing the fuel-air mixing and the combustion efficiency. Consequently, increased attention has been paid to such flows over the last 25 years through experimental, numerical and analytical studies, and many attributes of the flow have been explained (Lilley [1], Sloan et al. [2], Nallasamy [3]). The swirling motion imparted to the flow, either by a vane swirler or through a scroll, induces a radial pressure gradient and causes the pressure at the axis to fall. It results in an adverse pressure gradient along the axis, causing the formation of a central recirculating zone as a result of the vortex breakdown.

The properties of swirl stabilized flames are affected by the specific location of the reaction zone with respect to the recirculating velocity field (Gouldin et al. [4], Fujii et al. [5]). It is believed that the swirl flame tends to blow off if the reaction front fails to overlap the low speed flow region near the zero axial velocity line in the recirculation zone (Tangirala et al. [6]). Thus, the central recirculation in the combustor helps to stabilize the flame near the burner, overcoming the effect of blow-off due to the high velocity air jet. The location and size of the recirculation zone has, therefore, a very important bearing on the design of the combustor.

Though reaction and heat release in the combustor significantly alter the flow pattern (Tangirala et al. [6], Farag et al. [7]), comparative studies of isothermal flows can give an insight into certain behaviour of turbulent swirling flow in a combustor. Isothermal conditions offer a more favorable atmosphere to study and the relative influences of some parameters on the flow with and without combustion remain similar. For example, in case of a gas turbine combustor, the cold loss (i.e., pressure loss under isothermal conditions) is of the order of twenty inlet dynamic head, while the fundamental loss (i.e., additional pressure loss due to combustion) is only about one to two inlet dynamic head (Cohen et al., [8]). This delineates the importance of the cold flow study in the combustor. A lot of studies have been done without combustion both in the simplified combustor

* Corresponding author.
E-mail addresses: amdatta@hotmail.com (A. Datta), stutul@rediffmail.com (A. Sarkar).

1290-0729/$ – see front matter
doi:10.1016/j.ijthermalsci.2004.01.006

Nomenclature

D	diameter of the combustor
D_h	diameter of swirl generator hub
D_t	diameter of swirl generator tip
k	turbulent kinetic energy
L	length of the combustor
L_c	length of the central recirculation
L_w	axial distance of the position of maximum width of recirculation bubble from inlet
m	mass flow rate
m_r	recirculated mass flow rate in the central recirculation bubble
r	radial distance
R	radius of the combustor
R_h	radius of the swirler hub
R_t	radius of the swirler tip
S	swirl number defind at inlet plane
V	mean velocity
z	axial distance

Greek symbols

α	side wall expansion angle of the combustor
ε	dissipation rate of kinetic energy
ϕ	swirler vane angle
ρ	density
ψ	streamfunction

Subscripts

in	inlet plane
z	axial direction
θ	tangential direction

geometries, like dump combustors, and in complex, realistic geometries (Farag et al. [7], Green and Whitelaw [9], Rhode et al. [10,11], Ramos [12], Bicen and Jones [13], Yoo and So [14], Jones and Pascau [15], Koutmas and McGuirk [16], Nejad et al. [17], Favoloro et al. [18], McGuirk and Palma [19], Chang and Chen [20], Lin [21], Ahmed [22], Foster et al. [23]). Foster et al. [23] showed that under certain conditions the isothermal models give a very good account of the reacting flows.

The degree of swirl for a swirling flow is characterized by the swirl number, S, which is the ratio of the axial flux of angular momentum to the axial flux of axial momentum times a characteristic length (usually taken as the radius of the swirler). Swirl number at the inlet to the combustor (S) is one of the most important input parameter influencing the flow pattern in a turbulent swirling flow. For a low inlet swirl number, less than a critical value, no central recirculation is found. These are called weakly swirling flow. Beer and Chigier [24] reported the critical swirl number to be 0.6 for a simple pipe flow, exceeding which the flow is said to be a strongly swirling one with the appearance of the central recirculation zone. However, the critical swirl number depends on the flow geometry and may vary from the one prescribed by Beer and Chigier.

A lot of numerical results are now available on turbulent swirling non-reacting and reacting flows (reviewed by Sloan et al. [2], Nallasamy [2], Brewster et al. [25]). The critical part of the numerical model is the choice of a suitable turbulence closure model. It is probably one aspect on which a host of research papers have been published and a lot of conflicting opinions have been forwarded. It has been reported that the standard k–ε turbulence model has certain limitations in predicting swirling flows (Sloan et al. [2], Nallasamy [3], Koutmas and McGuirk [16], Favoloro et al. [18], Sturgess and Syed [26]). This is because the streamline curvature in the recirculating zones causes large changes in the higher order quantities of the turbulent structure, thereby, losing the isotropic structure of turbulence and also results in additional turbulence generation terms. Different ad-hoc modifications, with the introduction of additional empirical constants, are proposed by several researchers for an improved description of the swirling flow (Chang and Chen [20], Rodi [27], Srinivasan and Mongia [28]). But none of such modifications was found to work well under all kinds of geometries and for a wide range of swirl number. Another critical issue in the application of the k–ε model is the near wall treatment adjacent to the solid wall. Close to the wall, the local turbulent Reynolds number is small and molecular transport becomes important. Therefore, extremely fine mesh is to be adopted to resolve the near wall variables properly. As a result, the computational time increases considerably. Standard logarithmic wall functions are applied near the wall to overcome this problem by many researchers. Chang and Chen [20], Riahi et al. [29], Jiang and Shen [30] and Chen and Lin [31] adopted this approach for the solution of swirling flow using k–ε model in confined geometries. Alternately, Chen and Patel [32] suggested a two layer model, which is also used by Foster et al. [23] in their combustor flow field computation, for the treatment near the wall.

An attractive alternative to the problem is the use of higher order turbulence models, like the Algebraic Stress Model (ASM) and the Reynolds Stress Model (RSM). Some studies reported that, in swirling recirculating flows, the improvement of flow field predictions using the ASM were not so pronounced in comparison with those using the k–ε models (Sloan et al. [2], Chang and Chen [20], Sturgess and Syed [26]). RSM has been demonstrated to be capable of reproducing the major features of the swirling recirculating flow (Jones and Pascau [15], Fu et al. [33], Nikjooy and Mongia [34]), but it greatly increases the computational complex-

ity and time requirements. Lockwood and Shen [35] pointed out that very few numerical predictions of combusting systems have been made with the RSM model. Moreover, they found no consistent advantage of the RSM prediction over the standard k–ε results in their own investigation. Lin [21] showed that in predicting turbulent swirling flows, LES was better than the standard k–ε in the prediction of the scalar field, even though the velocity field predicted by the latter compares favorably with measurements.

Despite the advances in modeling turbulent flow, the standard k–ε model still remains a commonly used model in the prediction of turbulent reacting flows (Foster et al. [23], Datta [36], Gradinger et al. [37], Datta and Som [38], Tolpadi et al. [39]). Reacting flows, involving heat transfer, mass transfer and chemical reaction in addition to the fluid flow, are so complex that the deficiencies of the standard k–ε model is sacrificed compared to its advantages like simplicity and economy. Recently, in a review, Brewster et al. [25] commented that k–ε turbulence model is adequate in many cases for modeling in gas turbine combustors and the need for improved turbulence model is secondary to the need for more detailed chemical kinetics with improved modeling of chemistry/turbulence interaction. Many researchers, therefore, use the model in the prediction of isothermal flow in combustors too (Ramos [12], Foster et al. [23], Xia et al. [40], Dong and Lilley [41], Shyy et al. [42]). With such a background, the present model has also adopted the standard k–ε model for the solution of turbulent swirling flows.

The geometry of the combustor and the inlet conditions influence the flow pattern and the structure of the central recirculation zone, which are of prime importance in the design of combustion chambers. In a dump combustor geometry sudden expansion takes place right at the inlet plane. However, the actual geometry of the gas turbine combustors shows a gradual change in the cross-section through a diffuser at the entry. Rhode et al. [10,11] made a systematic study of the effect of side wall expansion angle of the diffuser along with the variation of the vane angle of the inlet swirler. They observed that the variation in side wall expansion angle affects the velocity distribution only at a high inlet swirl number and in a region close to the inlet. The recirculation zones are depicted through streamline plots. However, they did not evaluate the effect of the geometry on the location and size of the recirculation.

The effect of variations in inlet boundary conditions on flow has been studied by different reserachers. Ramos [12] and Sturgess et al. [43] showed that the numerical simulations of flows are highly sensitive to the inlet boundary conditions. Ikeda et al. [44] conducted experimental and numerical studies of flows in a model combustor and also showed that the flow is sensitive to inlet conditions. Dong and Lilley [41] studied the isothermal flow in an axi-symmetric combustor with emphasis on the influence of the inlet flow parameters. They observed that for the more accurate numerical prediction of the flow, the measured inlet profiles should be fed at the inlet boundary. Xia et al. [40] considered a combustor, where the inlet is oblique to the axis of the chamber, and studied the effect of radial velocity component at the inlet on the flow pattern. They found a significant contribution and defined a radial number analogous to the swirl number. Foster et al. [23] studied the isothermal analogue of combustion system with and without swirl. They found the accuracy of representation of the isothermal flows depends upon swirl number and concluded that the isothermal models produce a good account of the combusting flow at low swirl and small ratios of burner radius to combustion chamber radius. Though swirl number has been established as a significant input parameter contributing to the flow pattern, the effect of different types of swirl generators, maintaining the same swirl number, should also be an interesting aspect to study. Swirlers can be designed with different vane shapes. Most numerical works consider constant angled vanes for the calculations. But swirlers may be constructed with continuous variation of vane angle from the hub to the tip in the form of a helix, called a helicoidal vane swirler. The vane angle ϕ at any radius r for such a swirler can be expressed as

$$\phi = \tan^{-1}\left(\frac{r}{R_t}\tan\phi_t\right) \tag{1}$$

where, R_t and ϕ_t are the radius and vane angle at the tip of the swirler, respectively. It is apparent from the literature survey that no report on the effect of type of swirler and characterization of the resulting recirculation zone has appeared so far.

The present work, therefore, aims to report some important aspects of the turbulent swirling flow in a swirl combustor numerically, viz. the effects of side wall expansion angle and that of types of swirler on the recirculating bubble and detail characterization of recirculating flow region. Straight and helicoidal vanes are compared. Swirl numbers are varied by varying the vane angles for all the cases. Variation of swirl number is made in the range 0.4–2.0. Particular attention has been focussed on the central recirculation zone and its quantification in terms of size, location and strength.

2. Theoretical

2.1. Physical problem

The physical problem deals with the solution of an isothermal, turbulent flow within the confined geometry of an axi-symmetric combustor (Fig. 1). The combustor has a diffuser part near the entry plane with a specified constant side wall expansion angle (α). When $\alpha = 90°$, the geometry resembles that of a dump combustor. A central blockage, simulating the presence of a fuel injector is considered at the entry plane. The air entry into the combustor is through an annular passage around the central fuel injector, in which the vane swirler is placed.

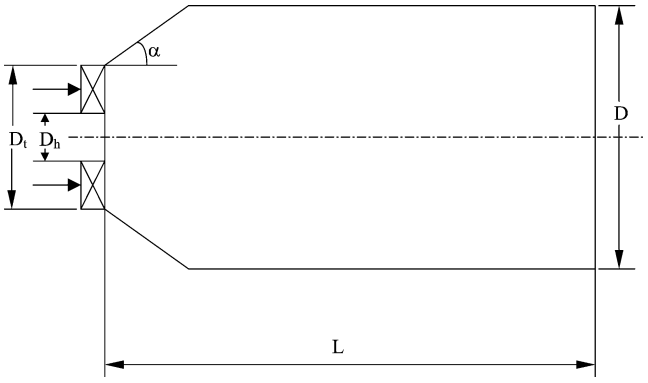

Fig. 1. Axi-symmetric combustor model.

The outer diameter of the combustor (D), diameter of the swirler tip (D_t) and that of the central injector (D_h) are considered to be 100, 50 and 20 mm, respectively. The diameter of the combustor has been chosen in the same order as reported by Ramos [12] and Cameron et al. [45] for model can combustors for gas turbines. The combustor length (L) is chosen as 1.0 m, so that the fully developed boundary condition, specified later, can be applied at the exit (Chang and Chen [20]).

2.2. Numerical model

A numerical model is developed for the solution of turbulent swirling flow using the standard k–ε model. It performs a simultaneous solution of the conservation of mass, momentum, turbulent kinetic energy and its dissipation rate equations within the physical domain. All the equations are written in cylindrical co-ordinates, considering symmetry about the axis. Standard empirical constants are employed for the k–ε solution.

The equations are discretized using an explicit finite difference technique with the variables defined in staggered grid arrangement. The diffusive terms in the conservation equations are discretized following a central difference scheme, while the advective terms are discretized following the power law scheme. During the solution, first the momentum equations along with the k and ε equations are explicitly advanced over a time step, computed satisfying the stability criteria. While advancing the momentum equations, the turbulent viscosity ($\mu_t = c_\mu \rho k^2/\varepsilon$) is computed using the current values of k and ε. The velocity and pressure terms are corrected through the continuity equation using an iterative technique, following a version of the MAC based SOLA algorithm (Hirt and Cook [46]). The method is similar to the earlier ones of Datta and Som [38] and Datta [36] for reacting flows in similar geometries.

2.3. Boundary and operating conditions

Due to the elliptic nature of the governing equations, boundary conditions should be specified at all boundaries of the computational domain, i.e., the inlet, outlet, axis and wall of the combustor, for the three components of the velocity, k and ε. At the inlet plane, the axial velocity has been considered to be uniform, while the radial velocity has been prescribed as zero. The local tangential velocity is computed using the local vane angle of the swirler as

$$V_{\theta|\text{in}} = V_{z|\text{in}} \tan\phi \tag{2}$$

In the case of a straight vane, the value of ϕ is considered to be constant over the entire inlet plane. However, for the helicoidal vane a variation in vane angle is considered following Eq. (1).

Inlet distributions of k and ε have been considered as

$$k_{|\text{in}} = 0.015(V_{z|\text{in}})^2 \tag{3}$$

$$\varepsilon_{|\text{in}} = \frac{(k_{|\text{in}})^{1.5}}{[0.005(R_t - R_h)]} \tag{4}$$

These correspond to a turbulent intensity of 10% of the inlet stream and an average turbulent length scale equal to 0.5% of the annulus height through which the flow enters the combustor. The chosen inlet values of turbulent intensity and length scale are consistent with those reported in earlier literatures (Foster et al. [23], Ramos [12]).

At the outlet, the axial gradient of all the variables have been set to zero as the length to diameter ratio of the chamber is chosen as 10. Symmetry condition has been adopted at the axis. No slip boundary condition is considered at the wall along with the logarithmic law of the wall.

In order to non-dimensionalize the governing equations, the combustor diameter (D) has been chosen as the characteristic length and the inlet axial velocity ($V_{z|\text{in}}$) is taken as the reference velocity. The mass flow rate of air is so chosen that the Reynolds number based on the inlet axial velocity ($V_{z|\text{in}}$) and the diameter of the combustor (D) is 65 600. This choice of Reynolds number is not arbitrary. In fact, it has been explicitly stated by Syred and Beer [47] that the Reynolds number of 20 000 can be considered to be large enough to ensure that the central vortex has broken down to form a well developed recirculation zone. Accordingly Tangirala et al. [6] carried out their experimental work with $Re = 20\,000$, with the air tube diameter as the characteristic length. Since, in the present case, the combustor diameter is chosen as the characteristic length, the Reynolds number, here, is much greater than the one stipulated by Syred and Beer [47] and is expected to bring out well developed central recirculations. The air is considered to be at room temperature. The vane angle of the swirlers are varied to study the impact of the inlet swirl strength and inlet swirl numbers of 0.4, 0.6, 0.8, 1.0, 1.2, 1.5 and 2.0 are considered. To study the effects of inlet vane type, solutions are made separately with the straight and the helicoidal vane swirlers in the geometry of 90° side wall expansion angle (α). In order to study the effect of side expansion angle, different cases with $\alpha = 90°$, 60°, 45° and 30° are considered. For each of these cases, the inlet swirl number is varied but the vane type has always been set as the straight one.

3. Results and discussion

3.1. Validation of the numerical code

The present numerical code is tested for its capability of predicting turbulent swirling flow by comparing its results against the experimental data of Dellenback [48] and the numerical predictions given in Chang and Chen [20] for standard k–ε model (Fig. 2(a) and (b)). The results of Dellenback, shown in the comparisons, are taken from the paper of Chang and Chen. The dump combustor geometry, as considered in the earlier works, has been chosen. The boundary conditions at the outlet, axis and wall are taken as prescribed by Chang and Chen. Chang and Chen computed the inlet boundary conditions from the inlet velocity profiles for the mean axial and tangential velocities by linearly extrapolating the data of Dellenback at z/D equal to -1.0 and -0.25. However, neither the computed inlet velocities nor the results of Dellenback upstream of the combustor are reported in the work of Chang and Chen. In the absence of suitable boundary data for the velocities, a uniform mean axial velocity and a corresponding mean tangential velocity produced by a constant-angled vane swirler are considered at the inlet. The mean radial velocities are taken as zero, as also adopted by Chang and Chen. The inlet-profiles of k and ε are considered following the prescriptions of Chang and Chen.

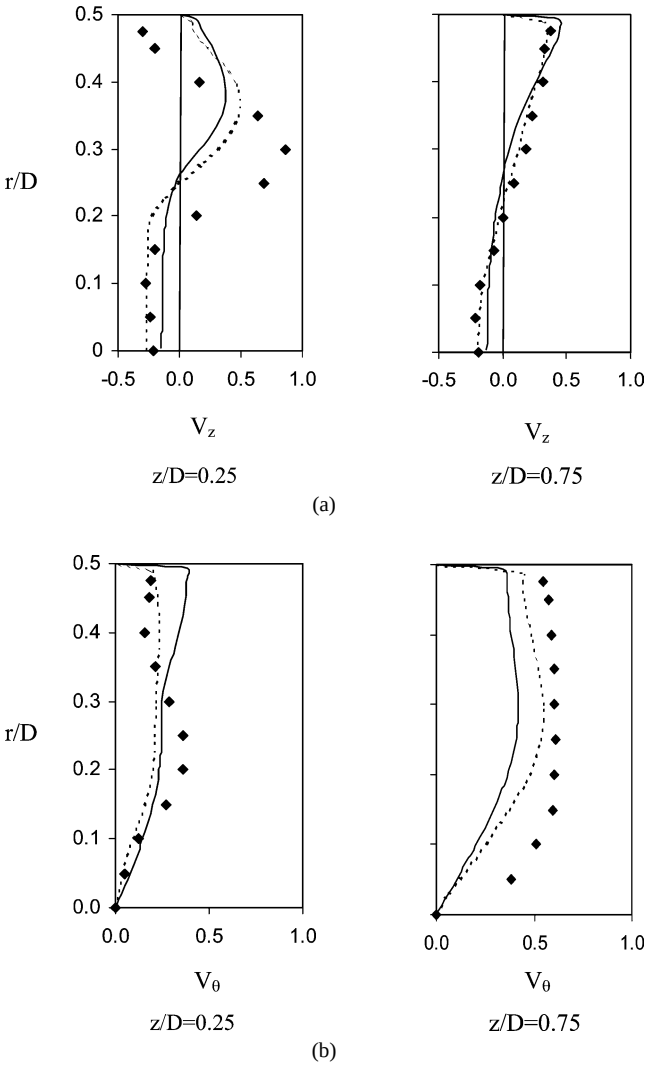

Fig. 2. (a) Comparison of mean axial velocity profiles at different axial locations as predicted by present model (—), standard k–ε model in Chang and Chen (- - -), and experiments of Dellenback (♦); (b) Comparison of mean tangential velocity profiles at different axial locations as predicted by present model (—), standard k–ε model in Chang and Chen (- - -), and experiments of Dellenback (♦).

Fig. 2(a) compares the radial variation of the mean axial velocities at different axial locations. The axial locations are chosen near the inlet for comparison ($z/D = 0.25$, and 0.75), as more spatial variations in the variables are observed in these regions. Fig. 2(a) shows that at the axial positions of z/D equal to 0.25, the mean axial velocity distributions from the present prediction are a little different from the predictions of Chang and Chen, and both differ from the experimental results. The differences among the results decrease in the downstream directions (e.g., at $z/D = 0.75$). One reason of the discrepancies in the predictions closer to the inlet are the differences in the inlet conditions adopted in the present work and that of Chang and Chen. However, once the influence of the inlet decreases, the two models predict similar distribution of the axial velocities. It is observed from the figures that both the model predictions differ from the experimental results in the quantitative sense. The models predict lower length of the central recirculation zone and also of the corner recirculation. The difference can be attributed both to the variation in inlet conditions and to the deficiency of the k–ε model in predicting the swirling flow, as discussed before. The greater discrepancy between the simulation and experiments, particularly near the inlet, points towards the streamline curvature due to the recirculation zones as the probable cause. However, in a qualitative sense, the models predict the axial velocity distributions quite well, as seen from the figure. Fig. 2(b) shows the variation of the mean tangential velocities at axial locations of z/D equal to 0.25, and 0.75. Qualitative agreement between the model predictions and experimental data are again observed.

3.2. Grid test for mesh independent solution

The physical domain for the present solution has already been described. A variable sized grid system is generated in the domain for the numerical calculation. To ensure mesh independent results, a series of trial solutions is conducted for several mesh configurations in the axial and radial directions, viz. 60×30, 60×40, 85×40, 85×60 and 120×60. In all the cases, the meshes are non-uniform in both directions and denser meshes are considered in regions of high gradients, e.g., near the inlet in the axial direction and near the axis, at the wall and at the location corresponding to the tip of the inlet swirler in the radial direction. Grid size in

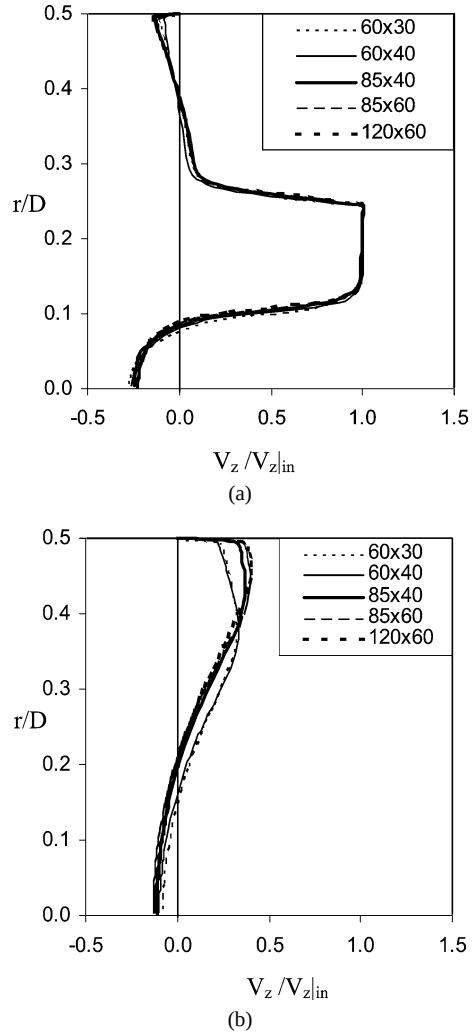

Fig. 3. Comparison of mean axial velocity profiles at different axial locations with various mesh configurations: (a) $z/D = 0.1$; (b) $z/D = 1.0$.

the radial direction is not varied monotonically. To resolve the strong gradient across the central recirculation zone very fine grids are considered near the axis. The grid size is also made fine at the outer (i.e., tip) radius of the inlet swirler and at the wall. However, under no circumstances the relative change in the consecutive grid size exceeds 15%.

Solutions are obtained for the geometry with $\alpha = 90°$ and a straight vane swirler, with the inlet swirl number equal to 0.4. Fig. 3(a) and (b) show the variations of the mean axial velocity profiles at two axial positions of $z/D = 0.1$ and 1.0 and Table 1 shows the maximum values of the stream-functions with their locations and the length of the central recirculation zones (L_c) for the different cases. The results show that at the position of $z/D = 0.1$, the axial velocities predicted with all the configurations are quite in agreement, except at a few radial locations. However, the grids of 60×30, 60×40 predict considerably different results from the others at $z/D = 1.0$. The maximum stream-functions are predicted within a variation of 2% in all the cases. In the last three cases, the difference is even less than 0.5%.

Table 1
Comparison of results for different mesh configurations

Mesh configuration	Maximum stream function and its location			L_c/D
	ψ_{max}	z/D	r/D	
60×30	0.03453	0.3234	0.4058	1.228
60×40	0.03428	0.3616	0.4045	1.251
85×40	0.03480	0.3372	0.4215	1.298
85×60	0.03494	0.3372	0.4148	1.310
120×60	0.03478	0.3448	0.4285	1.316

Similarly, the differences in the length of the recirculation zone as predicted in the last three configurations are within a maximum variation of 1%. Considering all these facts, 85×40 grid cells in the axial and radial directions respectively are considered as the optimum for the solutions in the present geometry and has been adopted for all the cases studied.

3.3. Flow patterns for different side expansion angle and vane type

Figs. 4–6 show the streamline patterns in one half of the axi-symmetric combustor for two different side expansion angles ($\alpha = 90°$ and 45°) and different swirler vane types (straight and helicoidal) with different inlet swirl numbers ($S = 0.4$ and 1.5). As the variations in the flow patterns are observed close to the inlet, the streamline plots are shown up to $z/D = 3.0$ in the axial direction in the figures.

Fig. 4(a) shows the flow pattern in a dump combustor ($\alpha = 90°$) with a straight vane swirler at the inlet, having a vane angle that results an inlet swirl number of 0.4. The figure reveals the formation of a corner recirculation zone and a central recirculation zone immediately downstream of the inlet. The corner recirculation is caused by the flow separation from the side wall of the combustor as the fluid stream enters, while, the central recirculation is the result of the adverse pressure gradient at the axis created by the swirl. The flowing stream of fresh fluid passes through the two recirculation bubbles with a high velocity till it spreads over the entire cross-section downstream of the recirculation zones. As the swirl number is increased to 1.5 (Fig. 4(b)), the central recirculation bubble grows in size both in the axial and radial directions and the maximum width of the recirculation occurs closer to the inlet. It reduces the corner recirculation zone considerably, and only a small corner bubble exists. The wider central recirculation zone leaves very little space near the periphery for the stream to flow, resulting in a higher stream velocity and longer recirculation length.

Fig. 5(a) and (b) show the effects of the side expansion angle on the flow patterns. The swirl numbers and vane types are kept the same as in Fig. 4(a) and (b), respectively. For a low swirl number ($S = 0.4$), Figs. 4(a) and 5(a) reveal that the change in geometry has little effect on the flow, except that the corner recirculation zone is curtailed by the angled wall in the second case with $\alpha = 45°$. The central part does not show any effect due to the change in geometry.

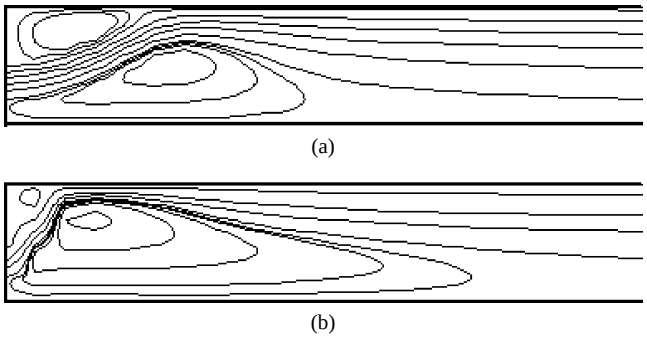

(a)

(b)

Fig. 4. Predicted streamline plots in combustor up to a length $z/D = 3.0$, with side wall expansion angle $\alpha = 90°$ and straight vane type swirl generator with swirl numbers (a) $S = 0.4$, (b) $S = 1.5$.

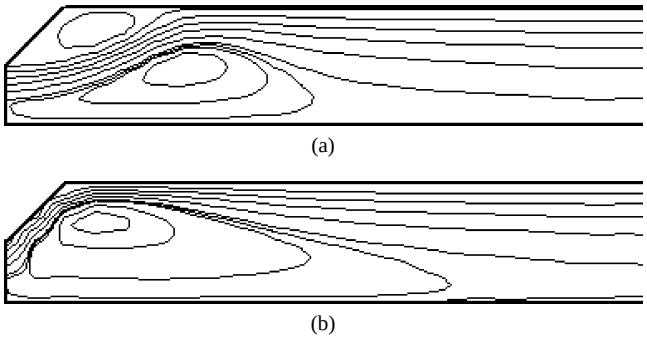

(a)

(b)

Fig. 5. Predicted streamline plots in combustor up to a length $z/D = 3.0$, with side wall expansion angle $\alpha = 45°$ and straight vane type swirl generator with swirl numbers (a) $S = 0.4$, (b) $S = 1.5$.

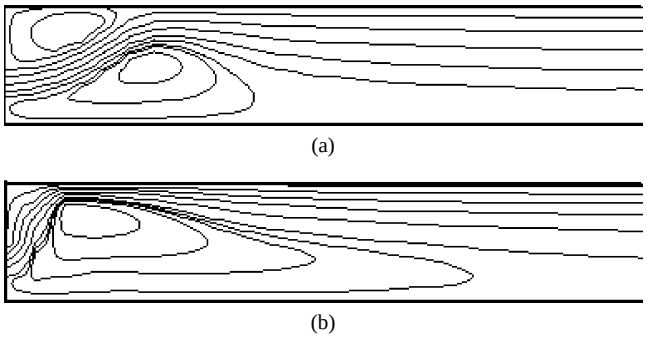

(a)

(b)

Fig. 6. Predicted streamline plots in combustor up to a length $z/D = 3.0$, with side wall expansion angle $\alpha = 90°$ and helicoidal vane type swirl generator with swirl numbers (a) $S = 0.4$, (b) $S = 1.5$.

However, as the swirl number is increased ($S = 1.5$), some differences in the flow patterns are observed with a change in α (Figs. 4(b) and 5(b)). The small corner recirculation zone, which exists in the $\alpha = 90°$ combustor, disappears when α is reduced to 45°. The central recirculation zone reduces slightly in length. The disappearance of the corner recirculation is due to the fact that with the angled side wall, the flow stream deflected by the large central recirculation bubble, attaches to the wall. In fact, with a lower value of α it is possible to get rid of the corner recirculation even at a lower swirl number. Thus the variation in flow pattern with the change in side wall expansion angle is discernible for a strongly swirling flow and that only near the inlet. Rhode et al. [10,11] also obtained similar conclusions from their studies. The streamline plots shown by them reveal almost no dependence on α for $S = 0$ and 0.67, but considerable difference is observed for $S = 1.83$, when α is varied from 90° to 45°.

In a combustor the central recirculation zone has a definite role in stabilizing the flame near the zone of low velocity. However, the corner recirculation does not serve any positive purpose. On the contrary, the recirculation bubble at the wall does not enable the fresh cool stream of air to come in contact with the wall and may result in overheating the wall. Therefore, a corner or wall recirculation should be avoided with a proper choice of the geometry and flow.

Fig. 6(a) and (b) show the flow patterns obtained in a dump combustor geometry with helicoidal vane swirlers. The vane angles are so adjusted that the inlet swirl number can be maintained at 0.4 (Fig. 6(a)) and 1.5 (Fig. 6(b)), respectively. As for a helicoidal vane, the vane angle of the swirler varies from the hub to the tip, the vane angle at the hub is less and at the tip is more than that of a straight vane swirler with the same swirl number. Comparison of Figs. 4(a) and 6(a) show that such a change of the vane design does not change the flow pattern within the combustor considerably, when the inlet swirl number is low ($S = 0.4$). The central and the corner recirculating zones are of similar size and shape in both cases. However, when the swirl number is increased to 1.5, though the central recirculation zones are same for the two inlet vane types (Figs. 4(b) and 6(b)) but the corner recirculation has almost disappeared with the introduction of the helicoidal vane. When the swirl number is 1.5, the vane angle of the straight vane is 63.7°, while the vane angle at the tip for helicoidal vane is 68.9°. The increased vane angle at the tip increases the tangential velocity there, and deflects the flow more towards the outer periphery. This sheds off much of the corner recirculation with the helicoidal vane.

The above comparisons of the flow patterns for different side wall expansion angle and swirler vane type reveal that not much difference occur with either of the variations when the swirl number is low. At a high swirl number, considerable differences are observed for either a variation in the side wall expansion angle or the vane type, particularly at regions close to the inlet of the combustor. However, far in the downstream section, the influence of the variations is less pronounced and the flow is mostly dependent on the Reynolds and swirl numbers.

3.4. Distributions of mean and turbulent quantities

Though the streamline plots give an overall impression regarding the flow pattern, a more detailed observation can be obtained from the distributions of the mean and turbulent quantities along the combustor. Therefore, the radial distributions of the mean axial and mean tangential velocities and of turbulent kinetic energy at different axial

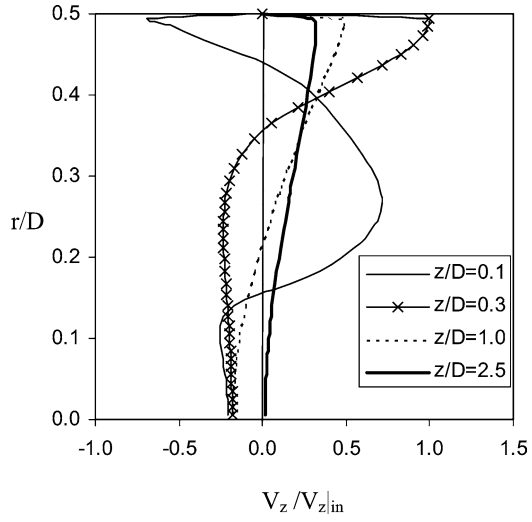

(a)

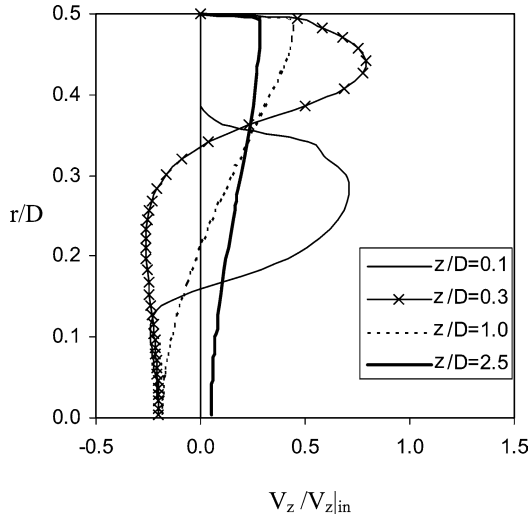

(b)

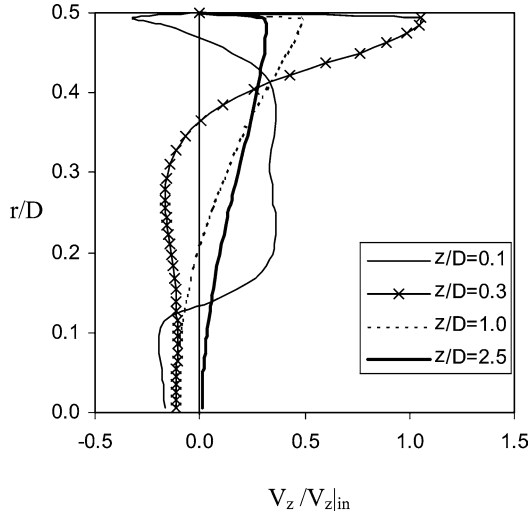

(c)

Fig. 7. Radial distribution of mean axial velocity at different axial locations in combustor with (a) $\alpha = 90^\circ$ and straight vane swirl generator, (b) $\alpha = 45^\circ$ and straight vane swirl generator, (c) $\alpha = 90^\circ$ and helicoidal vane swirl generator.

locations are plotted in Figs. 7–9 for different geometries and inlet swirl vanes. Comparisons are made with high swirl number only ($S = 1.5$), as the difference in the flow pattern is observed under that condition. Attention is focussed on the near-inlet region and four different axial stations at $z/D = 0.1$, 0.3, 1.0 and 2.5 are selected for the comparison.

The variations of the mean axial velocities for the different conditions are shown in Fig. 7(a), (b) and (c) for inlet swirl number of 1.5. Fig. 7(a) corresponds to $\alpha = 90^\circ$ and straight vane swirler, Fig. 7(b) is for $\alpha = 45^\circ$ and straight vane swirler, while Fig. 7(c) depicts the case for $\alpha = 90^\circ$ and helicoidal vane swirler. It can be observed from Fig. 7(a) that, at $z/D = 0.1$ the central recirculation zone exists, with the maximum reverse flow velocity at an off-axis location. The negative velocity gradually increases in magnitude from the axis to the radial location corresponding to its maximum and then changes to a positive value. The corner recirculation zone is small in width, but the magnitude of the reverse flow velocity component is high. The distribution at $z/D = 0.3$ shows that the maximum negative velocity in the central recirculation is off-axis and the width of the recirculation is very large. No corner recirculation persist at this location, as the size of the corner recirculation is small (Fig. 4(b)). On the contrary, a very high positive axial velocity is observed to exist close to the wall, from which the velocity sharply drops to zero at the wall. Rhode et al. [10] also reported such a high positive axial velocity close to the wall near the inlet (at $z/D = 0.3$) for high swirl number flow ($S = 1.83$). The distribution of the mean axial velocity begins to smoothen up in the downstream direction as observed at $z/D = 1.0$ and 2.5. At $z/D = 2.5$, the axial velocity at the centerline is almost zero, revealing the end of the central recirculation zone there. However, further development in the distribution of the mean axial velocity continues downstream with the increase in centerline velocity and decrease in velocity near the periphery.

Fig. 7(b) show the mean axial velocity profiles for a geometry with $\alpha = 45^\circ$ and with straight vane swirler at the inlet. Comparison of Fig. 7(a) and (b) shows that, some differences in the axial velocity profiles have been observed with the change in side expansion angle. The most noticeable amongst these is the distribution at $z/D = 0.3$, where the maximum velocity which has occurred with $\alpha = 45^\circ$ is less in magnitude and away from the wall compared to those with $\alpha = 90^\circ$. Such a change of the axial velocity distributions was also reported by Rhode et al. [10] at a similar axial location for high swirl number flow. When $\alpha = 45^\circ$, the centerline axial velocity at $z/D = 2.5$ is greater than zero, showing that the length of the central recirculation bubble is shorter for this case compared to that with when $\alpha = 90^\circ$, where the same is zero.

Fig. 7(c) describes the variations of mean axial velocity profiles for a helicoidal inlet vane swirler in a geometry with $\alpha = 90^\circ$. Comparison of the results with Fig. 7(a) reveals the effect of inlet vane type on the mean axial velocities. The mean axial velocity profile at $z/D = 0.1$ for a helicoidal

vane swirler is totally different from that for a straight vane swirler, particularly in the positive velocity region. While, for a straight vane swirler, the maximum axial velocity at this axial location occurs as a peak at a specific radial location, the axial velocity for a helicoidal vane swirler remains at or near maximum for a considerable radial distance. It then seems reasonable to conclude that the flow velocities outside the central recirculation zone is more or less uniform when a helicoidal swirl generator is used. Fig. 7(c) also shows a small negative velocity region near the wall at $z/D = 0.1$, thereby, indicating the presence of a very small corner recirculation zone, which is not evident from the streamline plot shown in Fig. 6(b). Both the width and strength of the corner recirculation zone are much less compared to those for a straight vane swirler. The difference in the mean axial velocity distribution with the change in the design of swirler is not much evident at stations downstream, and at $z/D = 1.0$ and 2.5, the distributions are almost the same for the two cases.

Fig. 8(a), (b) and (c) show the predicted mean tangential velocities at different axial positions under different conditions. From all the figures, it is evident that the variation in the tangential velocity distributions with side wall expansion angle or inlet vane type is only discernible near the inlet. In all the cases, at $z/D = 2.5$, a forced vortex like distribution is observed with the magnitude depending upon the inlet swirl intensity. At $z/D = 0.1$ in case of straight vane swirler and in a geometry with 90° side wall expansion angle, the maximum tangential velocity occurs as a peak at a particular radial position, and reduces with either increase or decrease in radius. At $z/D = 0.3$, the tangential velocity increases from zero at the axis to a high value following a forced vortex pattern. Then it decreases first, forming a trough, and increases again to show a high value near the wall. Subsequent transformation of the distribution, first into a combined vortex and then to a forced one takes place at $z/D = 1.0$ and 2.5, respectively.

Fig. 8(b) shows the mean tangential velocity distributions with $\alpha = 45°$ and straight vanes, while Fig. 8(c) depicts the distribution for $\alpha = 90°$ and helicoidal vanes. With the variation in the side wall angle, not much difference in the mean tangential velocities is observed at different axial locations from the earlier $\alpha = 90°$ cases for the same swirl numbers. A difference in the inlet vane type results in differences in the distribution very close to the inlet, viz. at $z/D = 0.1$. The differences, however, even out in the downstream locations and, at $z/D = 1.0$, similar distributions are observed both at low and high inlet swirls.

Fig. 9(a), (b) and (c) compare the turbulent kinetic energies predicted by the model for the different cases considered. It is to be noted that for all the cases under study the inlet values of k are the same. The variation in k values, as observed at different locations, is due to its generation and subsequent dissipation aided by the respective flow pattern. The predictions reveal that after the entry into the combustor, due to the formation of the recirculation zone

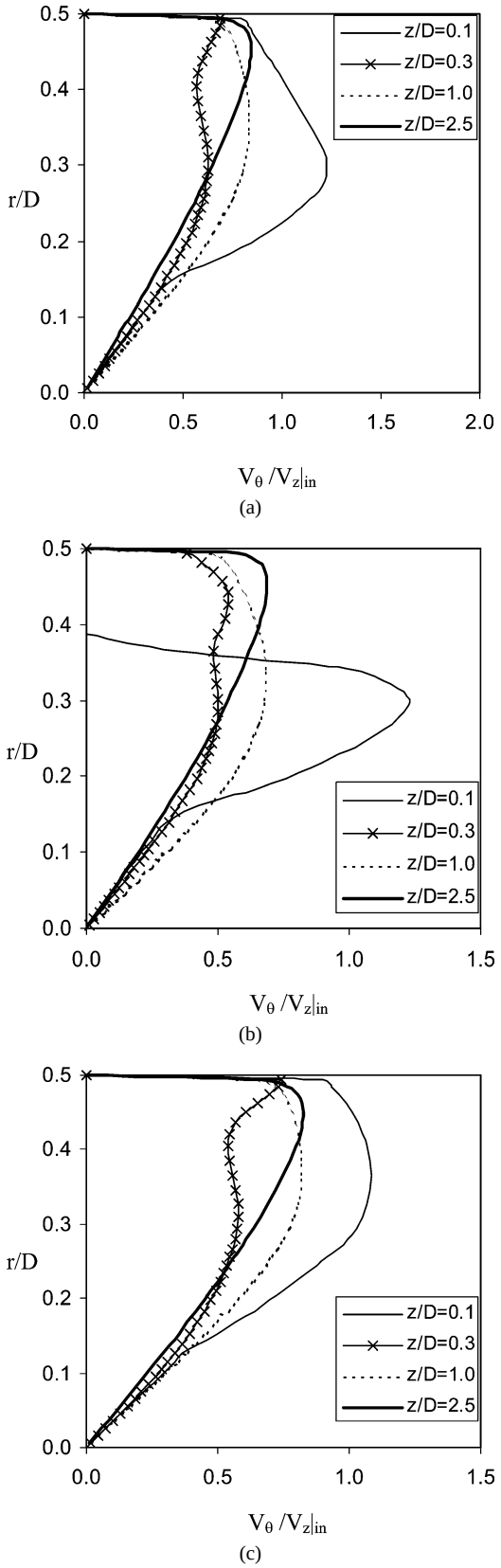

Fig. 8. Radial distribution of mean tangential velocity at different axial locations in combustor with (a) $\alpha = 90°$ and straight vane swirl generator, (b) $\alpha = 45°$ and straight vane swirl generator, (c) $\alpha = 90°$ and helicoidal vane swirl generator.

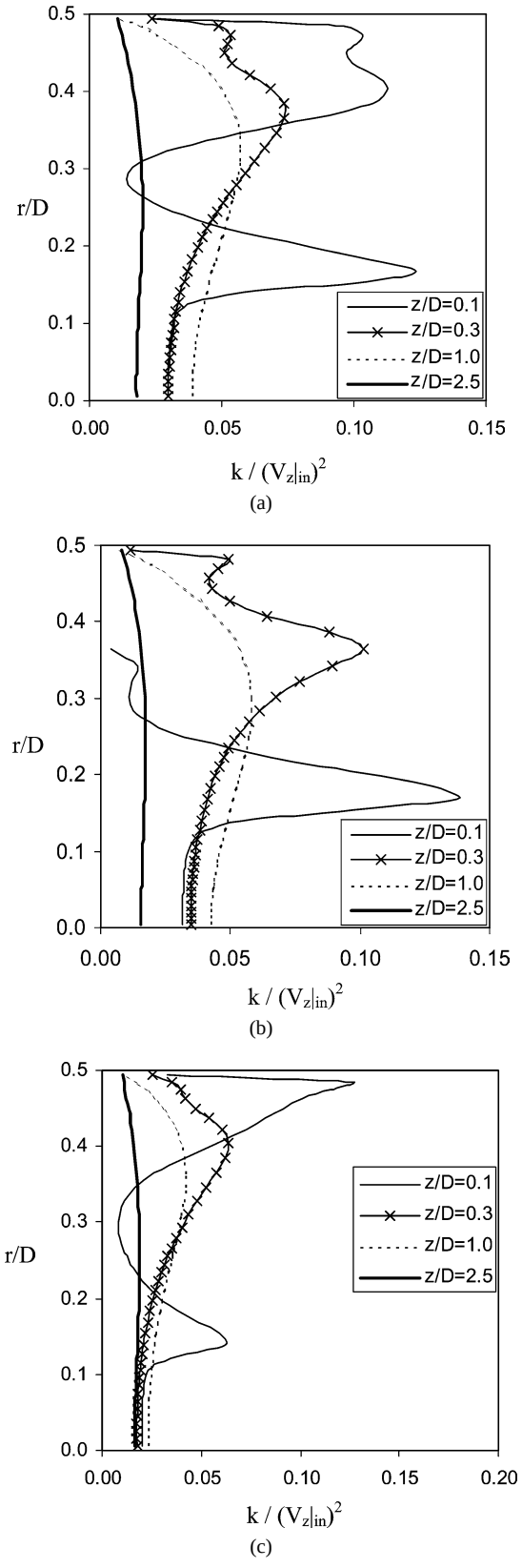

Fig. 9. Radial distribution of tangential kinetic energy at different axial locations in combustor with (a) $\alpha = 90^\circ$ and straight vane swirl generator, (b) $\alpha = 45^\circ$ and straight vane swirl generator, (c) $\alpha = 90^\circ$ and helicoidal vane swirl generator.

and the rapid increase of the axial and tangential velocity gradients, turbulent kinetic energy is generated and grows to large values at particular positions. A high value of k is observed at the radial location of the zero mean axial velocity within the central recirculation near the entry plane. When $\alpha = 90^\circ$ and straight vane swirler is in use, the maximum values of k at $z/D = 0.1$ and 0.3 occur at the radial location of zero mean axial velocity within the central recirculation (Fig. 9(a)). However, in this case, the maximum k at $z/D = 0.1$ far outweighs other k values. As the central recirculation grows faster with the high inlet swirl, the maximum width of the recirculation bubble occurs close to the inlet. So, the largest value of k is also closer to the inlet for the higher swirl number case. Nonetheless, it is evident that a high turbulence zone can be achieved in the central recirculation bubble near the inlet, where the axial velocity is low. This zone in the recirculation bubble is suitable for the combustion reaction. The low velocity obviates the blow-off of the flame while the high turbulence enhances the mixing process to support combustion.

A change in the side wall expansion angle from $\alpha = 90^\circ$ to $\alpha = 45^\circ$ does not make much change in the development and distribution of the turbulent kinetic energy at various axial locations. This is evident by comparing Fig. 9(b) against Fig. 9(a). However, comparison of Fig. 9(a) and (c) show that the introduction of helicoidal vanes, instead of the straight ones, results in some change in the distribution of k near the inlet, when the inlet swirl number is high. It is seen that with the helicoidal vane, the maximum k at $z/D = 0.1$ does not occur in the central recirculation zone, but near the wall (Fig. 9(c)). However, the value of k in the central recirculation still attains a smaller peak, which can help in enhancing the mixing process there. The smaller peak with the helicoidal vane is the result of the change in mean axial velocity distribution at the respective location. The almost flat profile in the mean axial velocity reduces the generation of k. At other axial locations the distribution of k does not show much effect of the variation in vane type.

3.5. Central recirculation zone

From the previous discussion on the flow pattern and the distributions of the mean and turbulent quantities, it is evident that the central recirculation has a major role to play in the combustor design. It helps in stabilization of the flame in the region of low velocity, where the increase in turbulence enhances the mixing process and increases the burning rate. The present work is only restricted to the isothermal cold flow within the combustor. However, a detailed study of the recirculation bubble with varying swirl intensity even for cold flow can throw important insight necessary for the reacting flow. The pertinent quantities regarding the central recirculation may be the size, position and strength of the recirculation zone.

The size and length of the recirculation zone may influence the position of the flame and the flame height. The size

of the recirculation zone can be expressed by its length. The central recirculation zone has been identified by the zero streamline, across which there is no net mass flow. The line originates from the edge of the central bluff body and meets the axis at the rear stagnation point. The distance of the rear stagnation point from the entry plane determines the length of the recirculation zone (L_c). The length can also be derived from the zero axial velocity contour within the recirculation bubble. This line meets the axis at the rear stagnation point along with the zero streamline. In fact the zero axial velocity line divides the recirculation bubble into two parts. Between the central axis and the zero axial velocity line is the region through which the recirculated mass flows backwards, i.e., towards the inlet. On the contrary, the recirculated mass moves forward through the region between the zero axial velocity line and the zero streamline. In all the cases the central recirculation originates from the inlet because of the presence of the central body. However, depending upon the inlet swirl number the recirculation grows differently. For higher swirl number flow, the maximum width of the recirculation bubble occurs closer to the inlet, indicating that the recirculation has moved towards the inlet plane. Thus, the position of the recirculation bubble is determined by the axial position corresponding to the maximum width of the recirculation bubble (L_w).

The strength of the recirculation is expressed by the mass of the gas recirculating in the central bubble. The strength is important because it decides the preheating ability of the fresh charge by the recirculating high temperature gas in the reacting flow situation in the combustor. However, too strong a recirculation may overheat the burner and shorten its life. Moreover, the presence of burnt gases in high concentration in the recirculated gas may limit the combustion reactions if the circulation is strong. The recirculating mass within the central bubble is different at different axial locations. At any axial location, the mass of fluid recirculated is obtained by integrating the quantity ($\rho \cdot V_z \cdot 2\pi r \, \mathrm{d}r$) from the centerline to the zero axial velocity line. The maximum value of this quantity within the central recirculation zone is considered as the rate of mass recirculated (m_r).

Fig. 10(a) and (b) show the variation of the length of the central recirculation bubble (L_c) with swirl number for varying side wall expansion angle and different swirler vane types respectively. The results show that for a low swirl number (0.4–0.8), the length of the recirculation zone does not change with the variation of side wall expansion in the range of $\alpha = 30^\circ$ to 90° for the present value of Reynolds number (Fig. 10(a)). However, for a swirl number of 1.0, differences are observed in the length with the variation of α. The length of the central recirculation is less when the side wall expansion angle is low, for the same swirl number. However, till a swirl number of 1.2, the increase in the recirculation length is not very different as the side wall expansion angle increases. For a swirl number of 1.5 and higher, the length of the recirculation in the combustor with $\alpha = 90^\circ$ increases very rapidly, much beyond the length in

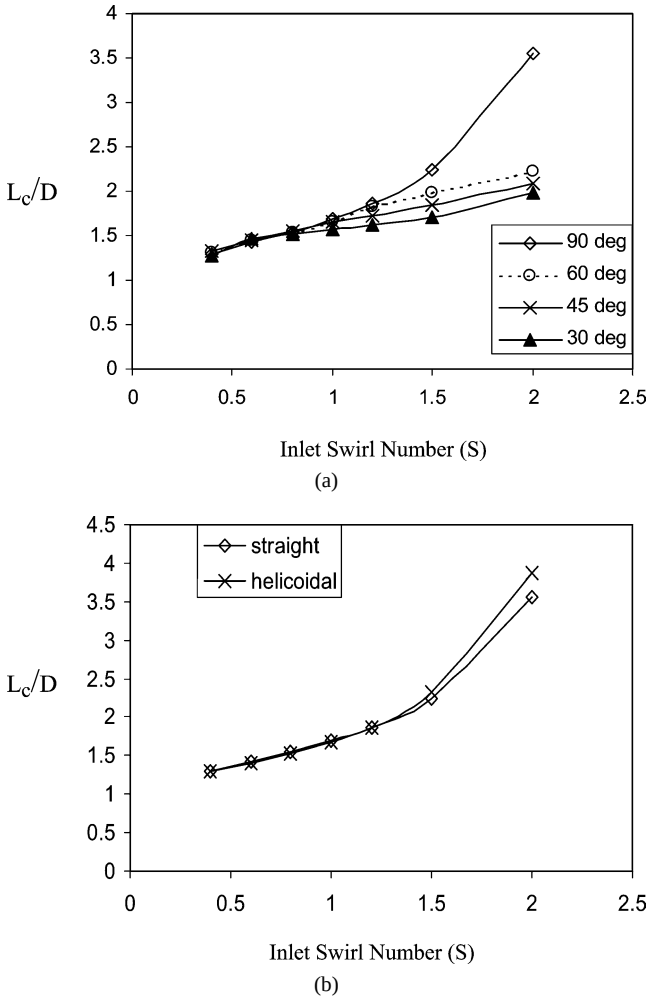

Fig. 10. (a) Variation of the length of the central recirculation zone (L_c) with inlet swirl number for different side wall expansion angle and straight vane swirl generator. (b) Variation of the length of the central recirculation zone (L_c) with inlet swirl number for different swirl generator vane type and side wall expansion angle $\alpha = 90^\circ$.

other geometries for the corresponding swirl numbers. The reason may be attributed to the fact that with the increase in swirl number the central recirculation bubble grows in width and moves closer to the inlet decreasing the size of the corner recirculation there. It leaves less space for the fluid stream to flow and increases its velocity. The high velocity stream displaces the rear stagnation point further downstream, thereby increasing the length of recirculation. In the case of a side expansion angle less than 90°, the flow does not separate from the side wall as the swirl number is increased beyond a particular value. After this, the recirculation bubble cannot grow in size or lengthen in the same proportion and becomes smaller than that in the dump combustor geometry. The variable vane type at the inlet does not have a strong influence on the recirculation length. The lengths of the recirculation length either with a straight vane or helicoidal vane are the same for the same swirl number, until the swirl number increases to 1.5. For $S = 1.5$, the length with helicoidal vane is slightly more than with the

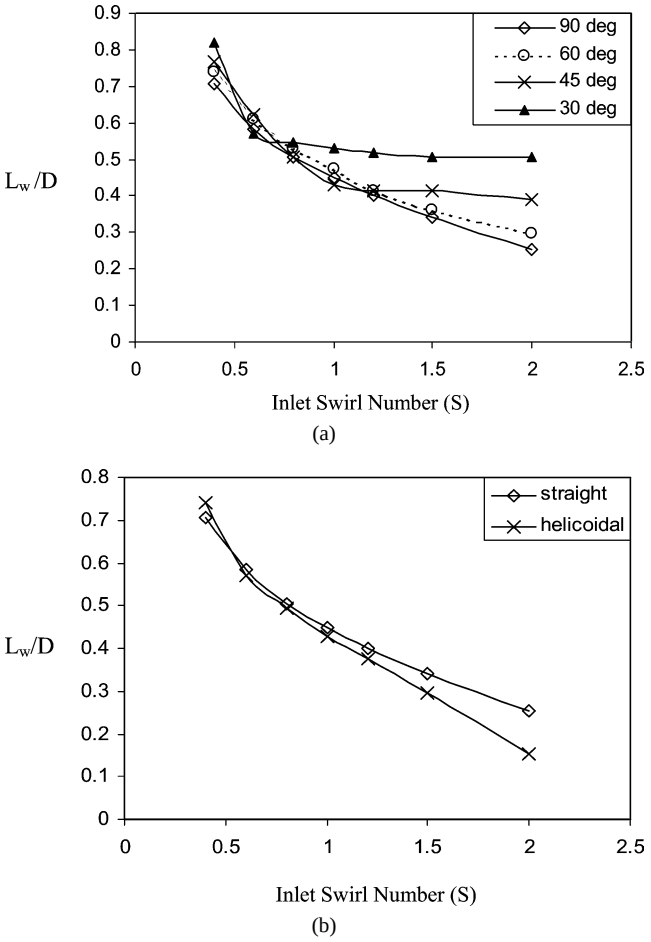

Fig. 11. (a) Variation of the axial distance of the maximum width of central recirculation zone from the inlet with inlet swirl number for different side wall expansion angle and straight vane swirl generator; (b) Variation of the axial distance of the maximum width of central recirculation zone from the inlet (L_w) with inlet swirl number for different swirl generator vane type and side wall expansion angle $\alpha = 90°$.

straight vane. The difference is even larger at $S = 2.0$. The vane angle with a high swirl number is high. However, with the helicoidal vane, the vane angle at the tip is even more. The higher vane angle at the tip increases the tangential velocity and increases the recirculation bubble further. This increases the length of the central recirculation zone.

Fig. 11(a) and (b) show the variation of the axial distance of maximum width of the recirculation zone from the inlet (L_w) as function of the swirl number for various geometries and vane types respectively. The variation of the side wall expansion angle (α) has an interesting effect on L_w at different swirl numbers. When α is 90° or 60°, L_w continuously decreases with the increase in the swirl number in the range of 0.4–2.0. However, for smaller values of α, like 45° or 30°, L_w decreases with increase in swirl number up to certain point, beyond which L_w remains constant with further increase in the swirl number. The critical swirl number, beyond which L_w does not change, is less for $\alpha = 30°$ than for 45°. This may be attributed to the same reason as described earlier for the variation of recirculation length. With the increase of the swirl number, the recirculation bubble moves upstream and the maximum width occurs closer to the inlet. Thus L_w decreases. When the side expansion angle is low, the flow does not separate at the side wall with the increase in the inlet swirl intensity. The corner recirculation vanishes. From this point onward, with the increase in swirl number, the central recirculation reduces moving upstream by any significant amount and L_w does not change. As the side wall expansion angle decreases, the flow ceases to separate from the side wall at a lower swirl number. Therefore, the variation in L_w is observed up to $S = 0.6$ when $\alpha = 30°$, but for $\alpha = 45°$, L_w changes with swirl number till $S = 1.0$. Thus, as the side wall of the combustor is sloped at an angle of 45° or less, a high swirl intensity can be reached with sufficient increase in the inlet swirl strength, without the central recirculation getting too close to the inlet or too long in the downstream direction. It is important to have such a control on the recirculation zone in the combustor. A recirculation too close to the inlet will draw the flame closer to the burner, which can overheat the burner itself. On the other hand, too long a recirculation zone may not be adequate for combustion and has negative effects on combustion efficiency and emissions. Fig. 11(b) shows the variation of L_w with the swirl number for two different vane types. The results show that for a low swirl number of 0.4, L_w is longer for the helicoidal vane, while for all other higher swirl numbers straight vanes give higher L_w. The difference is not appreciable, however, until the swirl number is very high, e.g., 1.5 or 2.0.

The other important parameter in the recirculation bubble is its strength, given by the mass recirculated. Fig. 12(a) shows the variation of (m_r/m_{in}) with swirl number for different side wall expansion. As the inlet mass flow rate is the same for all the cases, the ratio directly shows the variation of the recirculated mass. The figure shows that the ratio increases with the increase in swirl number for every geometry considered. For a low swirl number like $S = 0.4$, the ratio of (m_r/m_{in}) is between 0.1–0.2, showing a very low strength of the recirculation. But, as the swirl number is increased to 2.0, the ratio increases to a value near 0.5. For the geometries with $\alpha = 90°$, 60° and 45°, the recirculated mass is the same for the same swirl number, until the swirl number is as high as 2.0. At $S = 2.0$, the figure shows that the recirculated mass is maximum for $\alpha = 60°$, while it is less either with $\alpha = 90°$ or 45°. This shows the existence of a critical side expansion angle, when the recirculated mass is the maximum at high swirl intensity. The recirculated mass with $\alpha = 30°$ is, however, much less than that with any other α at all swirl numbers considered. The influence of vane type on the recirculated mass is somewhat more interesting (Fig. 12(b)). Though the size of the recirculation zone and its position are not very different with either the straight or helicoidal vanes, the recirculated mass with the helicoidal vane swirler is always less than that with the straight vane swirler for the same swirl number. The difference is low at very small swirl number ($S = 0.4$), but continues to increase

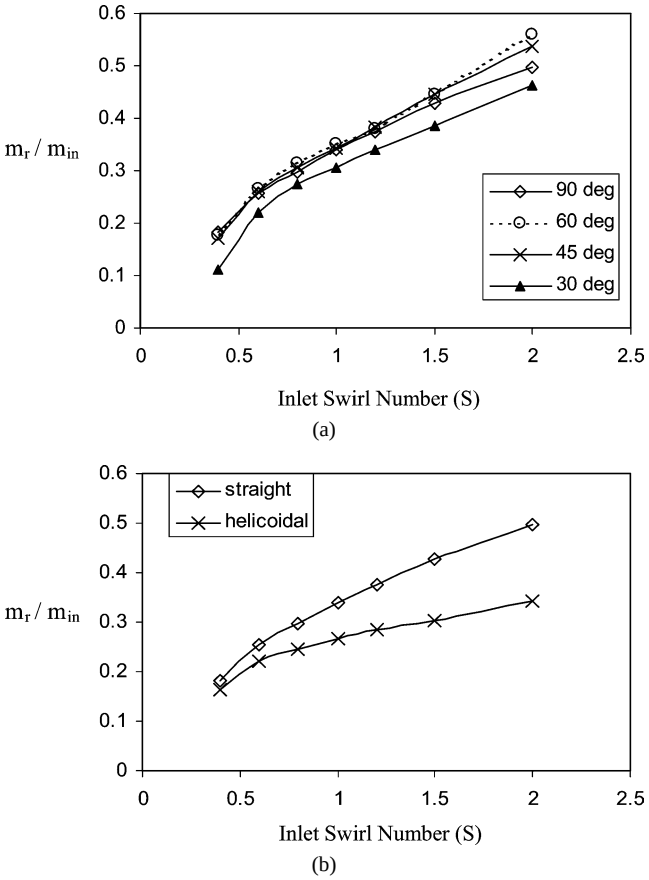

Fig. 12. (a) Variation of recirculated mass within the central recirculation zone with inlet swirl number for different side wall expansion angle and straight vane swirler generator; (b) Variation of recirculated mass within the central recirculation zone with inlet swirl number for different swirl generator vane type and side wall expansion angle $\alpha = 90°$.

as the swirl number increases and is more than 45% for $S = 2.0$. This is an interesting difference in the effect of vane type on the recirculation bubble, which may be of interest to the designers.

4. Conclusions

The present work has studied the isothermal turbulent swirling flow in an axi-symmetric combustor and observed the effects of side wall expansion angle of the inlet diffuser section and the vane type of the inlet swirler on the flow pattern and central recirculation bubble for a wide range of swirl numbers. The following conclusions can be drawn after the detailed analysis:

- The variations in the side wall expansion angle and the type of vane modifies the flow pattern in the combustor only at high swirl numbers and then near the inlet of the combustor. The influence of either of these variables at low swirl numbers is almost negligible. These can be concluded from the overall streamline pattern and from the mean axial and tangential velocity distributions near the inlet.
- The length of the central recirculation zone increases with swirl number for all the geometries studied. However, in a dump combustor, the length can be even three times or more at sufficiently high swirl numbers. Such a long recirculation has not been observed when the side wall expansion angle is reduced. The length of the central recirculation zone does not change with the use of helicoidal vane geometry compared to that with the straight vane geometry, unless the swirl number is very large.
- The axial position of the maximum width from the inlet section decreases as the swirl number is increased. However, when the side wall expansion angle is reduced to 45°, this does not change beyond a swirl number of 1.0. With further reduction in the side expansion angle to 30°, the maximum width position does not change even beyond a swirl number of 0.6. The axial position of the maximum width is almost always a little closer to the inlet with the helicoidal vane swirler than with the straight vane swirler. The difference somewhat increases with an increase in swirl number.
- The strength of the central recirculation increases as the swirl number increases, and more mass is found to circulate in the recirculation bubble. At a very high inlet swirl number, an optimum side expansion angle may be observed for which the strength of the recirculation is the maximum. When the side expansion angle is very low, the recirculation strength is found to be less at all swirl numbers. With the helicoidal vane at the inlet, the central recirculation is always less in strength than with the straight vane swirler.

References

[1] D.G. Lilley, Swirl flows in combustion: A review, AIAA J. 15 (8) (1977) 1063–1078.
[2] D.G. Sloan, P.J. Smith, L.D. Smoot, Modeling of swirl in turbulent flow systems, Prog. Energy Combust. Sci. 12 (1986) 163–194.
[3] M. Nallasamy, Turbulence models and their applications to the prediction of internal flows: A review, Computers Fluids 15 (2) (1987) 151–194.
[4] F.C. Gouldin, J.S. Depsky, S.L. Lee, Velocity field characteristics of a swirling flow combustor, AIAA J. 23 (1) (1985) 95–101.
[5] S. Fujii, K. Eguchi, M. Gomi, Swirling jets with and without combustion, AIAA J. 19 (6) (1981) 1438–1444.
[6] V. Tangirala, R.H. Chen, J.F. Driscoll, Effect of heat release and swirl on the recirculation within swirl-stabilized flames, Combust. Sci. Tech. 51 (1987) 75–95.
[7] T.M. Farag, M. Shimizu, M. Arai, Flow measurement in a swirl combustor in two cases with and without combustion, Bull. JSME 27 (225) (1984) 521–528.
[8] H. Cohen, G.F.C. Rogers, H.I.H. Saravanamuttoo, Gas Turbine Theory, second ed., Longmann, London, 1972.
[9] A.S. Green, J.H. Whitelaw, Isothermal models of gas turbine combustors, J. Fluid Mech. 126 (1983) 399–412.

[10] D.L. Rhode, D.G. Lilley, D.K. McLaughlin, On the prediction of swirling flowfields found in axisymmetric combustor geometries, J. Fluids Engrg. Trans. ASME 104 (1982) 378–384.
[11] D.L. Rhode, D.G. Lilley, D.K. McLaughlin, Mean flowfields in axisymmetric combustor geometries with swirl, AIAA J. 21 (4) (1983) 593–600.
[12] J.I. Ramos, Turbulent nonreacting swirling flows, AIAA J. 22 (6) (1984) 846–848.
[13] A.F. Bicen, W.P. Jones, Velocity characteristics of isothermal and combusting flows in a model combustor, Combust. Sci. Tech. 49 (1986) 1–15.
[14] G.J. Yoo, R.M.C. So, Variable density effects on axisymmetric sudden expansion flows, Internat. J. Heat Mass Transfer 32 (1) (1989) 105–120.
[15] W.P. Jones, A. Pascau, Calculation of confined swirling flows with a second moment closure, J. Fluids Engrg. Trans. ASME 111 (1989) 248–255.
[16] P. Koutmas, J.J. McGuirk, Isothermal modeling of gas turbine combustors: Computational study, J. Propulsion Power 7 (1991) 1064–1091.
[17] A.S. Nejad, S.P. Vanka, S.C. Favoloro, M. Samimy, C. Langenfeld, Application of laser velocimetry for characterization of confined swirling flow, J. Engrg. Gas Turbine Power Trans ASME 111 (1989) 36–45.
[18] S.C. Favoloro, A.S. Nejad, S.A. Ahmed, Experimental and computational investigation of isothermal swirling flow in an axisymmetric dump combustor, J. Propulsion Power 7 (1991) 348–356.
[19] J.J. McGuirk, J.M.L.M. Palma, The flow inside a model gas turbine combustor: Calculations, J. Engrg. Gas Turbine Power Trans. ASME 115 (1993) 594–602.
[20] K.C. Chang, C.S. Chen, Development of a hybrid k–ε turbulence model for swirling recirculating flows under moderate to strong swirl intensities, Internat. J. Numer. Methods Fluids 16 (1993) 421–443.
[21] C.A. Lin, Modeling a confined swirling coaxial jet, Centre for Turbulence Research, Annual Research Brief (1998) 211–219.
[22] S.A. Ahmed, Velocity measurements and turbulence statistics of a confined isothermal swirling flow, Experimental Thermal Fluid Sci. 17 (1998) 256–264.
[23] P.J. Foster, J.M. Macinnes, F. Schubnell, Isothermal modelling of a combustion system with swirl: A computational study, Combust. Sci. Tech. 155 (2000) 51–74.
[24] J.M. Beer, N.A. Chigier, Combustion Aerodynamics, Applied Science Publisher, London, 1972.
[25] B.S. Brewster, S.M. Cannon, J.R. Farmer, F. Meng, Modeling of lean premixed combustion in stationary gas turbines, Prog. Energy Combust. Sci. 25 (1999) 353–385.
[26] G.J. Sturgess, S.A. Syed, Calculation of confined swirling flows, Internat. J. Turbo Jet Engines 7 (1990) 103–121.
[27] W. Rodi, Influence of buoyancy and rotation on equations for the turbulent length scale, in: Proc. 2nd Symp. Turbulent Shear Flows, Imperial College, London, 1979, pp. 10.37–10.42.
[28] R. Srinivasan, H.C. Mongia, Numerical computation of swirling recirculating flows, Final report NASA CR-165196, 1980.
[29] A. Riahi, M. Salcudean, P.G. Hill, Computer simulation of turbulent swirling flows, Internat. J. Numer. Methods Engrg. 29 (1990) 533–557.
[30] T.L. Jiang, C.H. Shen, Numerical predictions of the bifurcation of confined swirling flows, Internat. J. Numer. Methods Fluids 19 (1994) 961–979.
[31] J.C. Chen, C.A. Lin, Computations of strongly swirling flows with second moment closures, Internat. J. Numer. Methods Fluids 30 (1999) 493–508.
[32] H.C. Chen, V.C. Patel, Near wall turbulence models for complex flows including separation, AIAA J. 26 (6) (1988) 641–648.
[33] S. Fu, P.G. Huang, B.E. Launder, M.A. Leschziner, A comparison of algebraic and differential second moment closures for axisymmetric turbulent shear flows with and without swirl, J. Fluids Engrg. Trans. ASME 110 (1988) 216–221.
[34] M. Nikjooy, H.C. Mongia, A second order modeling study of confined swirling flow, Internat. J. Heat Fluid Flow 12 (1991) 12–19.
[35] F.C. Lockwood, B. Shen, Performance predictions of pulverised-coal flames of power station furnaces and cement kiln types, in: Twenty Fifth (Int.) Symp. On Combustion, The Combustion Inst., Pittsburgh, 1994, pp. 503–509.
[36] A. Datta, Influence of inlet flow conditions on the performance of a swirl-stabilized combustor burning liquid fuel spray, Internat. J. Energy Res. 24 (2000) 373–390.
[37] T.B. Gradinger, A. Inauen, R. Bombach, B. Käppeli, W. Hubschmid, K. Boulouchos, Liquid-fuel/air premixing in gas turbine combustors: Experiment and numerical simulation, Combust. Flame 124 (2001) 422–443.
[38] A. Datta, S.K. Som, Thermodynamic irreversibilities and second law analysis in a spray combustion process, Combust. Sci. Tech. 142 (1999) 29–54.
[39] A.K. Tolpadi, D.L. Burrus, R.J. Lawson, Numerical computation and validation of two-phase flow downstream of a gas turbine combustor dome swirl cup, J. Engrg. Gas Turbine Power Trans. ASME 117 (1995) 704–712.
[40] J.L. Xia, B.L. Smith, A.C. Benim, J. Schmidli, G. Yadigaroglu, Effect of inlet and outlet boundary conditions on swirling flows, Comput. Fluids 26 (8) (1997) 811–823.
[41] M. Dong, D.G. Lilley, Effects of inlet velocity profiles on downstream flow development of turbulent swirling flows, in: Proc. of the 28th Intersoc. Energy Conversion Engineering Conference, vol. 1, 1993, pp. 707–714.
[42] W. Shyy, S.M. Correa, M.E. Braaten, Computation of flow in a gas turbine combustor, Combust. Sci. Tech. 58 (1988) 97–117.
[43] G.J. Sturgess, S.A. Syed, K.R. McMaus, Importance of inlet boundary conditions for numerical simulation of combustor flows, Paper AIAA-83-1263, 1983.
[44] Y. Ikeda, Y. Yanagisawa, S. Hosokawa, T. Nakajima, Influence of inlet conditions on the flow in a model gas turbine combustor, Experimental Thermal Fluid Sci. 5 (1992) 390–398.
[45] C.D. Cameron, J. Brouwer, C.P. Wood, G.S. Samuelson, A detailed characterization of the velocity and thermal fields in a model can combustor with wall jet injection, J. Engrg. Gas Turbine Power Trans. ASME 111 (1989) 31–35.
[46] C.W. Hirt, J.L. Cook, Calculating three-dimensional flows around structures and over rough terrain, J. Comput. Phys. 10 (1972) 324–341.
[47] N. Syred, J.M. Beer, Combustion in swirling flows: A review, Combust. Flame 23 (1974) 143–201.
[48] P.A. Dellenback, Heat Transfer and velocity measurements in turbulent swirling flow through an abrupt axisymmetric expansion, Ph.D. Thesis, Arizona State University, Tempe, Arizona, 1986.